# Search for astrophysically important $^{19}$Ne levels with a thick-target $^{18}$F$(p,p)^{18}$F measurement

D. W. Bardayan,[1] J. C. Blackmon,[1] J. Gómez del Campo,[1] R. L. Kozub,[2] J. F. Liang,[1] Z. Ma,[3] L. Sahin,[4,5] D. Shapira,[1] and M. S. Smith[1]
[1]*Physics Division, Oak Ridge National Laboratory, Oak Ridge, Tennessee 37831, USA*
[2]*Department of Physics, Tennessee Technological University, Cookeville, Tennessee 38505, USA*
[3]*Department of Physics and Astronomy, University of Tennessee, Knoxville, Tennessee 37996, USA*
[4]*Department of Physics and Astronomy, University of North Carolina, Chapel Hill, North Carolina 27599, USA*
[5]*Department of Physics, Dumlupinar Univ., Kutahya, Turkey 43100*
(Received 18 March 2004; published 21 July 2004)

The rates of the $^{18}$F$(p,\alpha)^{15}$O and $^{18}$F$(p,\gamma)^{19}$Ne reactions in astrophysical environments depend on the properties of $^{19}$Ne levels above the $^{18}$F$+p$ threshold. There are at least eight levels in the mirror nucleus $^{19}$F for which analogs have not been observed in $^{19}$Ne in the excitation energy range $E_x=6.4-7.6$ MeV. These levels may significantly enhance the $^{18}$F$+p$ reaction rates, and thus we have made a search for these levels by measuring the $^{1}$H$(^{18}$F$,p)^{18}$F excitation function over the energy range $E_{\mathrm{c.m.}}=0.3-1.3$ MeV. We have identified and measured the properties of a newly observed level at $E_x=7.420\pm0.014$ MeV, which is most likely the mirror to the $J^{\pi}=\frac{7}{2}^{+}$ $^{19}$F level at 7.56 MeV. We have additionally found a significant discrepancy with a recent compilation for the properties of a $^{19}$Ne state at $E_x=7.5$ MeV and set upper limits on the proton widths of missing levels.

DOI: 10.1103/PhysRevC.70.015804 PACS number(s): 27.20.+n, 25.40.Cm, 25.60.−t, 26.30.+k

## I. INTRODUCTION

The proton-induced reactions on $^{18}$F are of astrophysical interest for a variety of reasons. The amount of the long-lived radioisotope $^{18}$F [1,2] produced in novae depends critically on the rates of the $^{18}$F$(p,\alpha)^{15}$O and $^{18}$F$(p,\gamma)^{19}$Ne reactions [3]. The synthesis of other isotopes (e.g., $^{16}$O, $^{18}$O, and $^{19}$F) also show a dramatic sensitivity to the rates of these reactions [4]. In higher-temperature environments such as x-ray bursts, there may be a transition to heavy element production via the reaction sequence $^{18}$F$(p,\gamma)^{19}$Ne$(p,\gamma)^{20}$Na$(p,\gamma)^{21}$Mg… [5]. Whether there is a significant flow through this reaction sequence depends sensitively on the competition between the $^{18}$F$(p,\gamma)^{19}$Ne and $^{18}$F$(p,\alpha)^{15}$O reactions, and thus we must know their relative rates in these high-temperature astrophysical environments.

To accurately calculate the rates of the $^{18}$F$(p,\alpha)^{15}$O and $^{18}$F$(p,\gamma)^{19}$Ne reactions, we must understand the level structure of $^{19}$Ne above the proton threshold at $E_x=6.411$ MeV. Despite numerous stable [6,7] and radioactive [8–12] beam studies of $^{19}$Ne, there still exist at least 8 levels in the mirror nucleus, $^{19}$F, for which analogs have not been observed in $^{19}$Ne in the excitation energy range $E_x=6.4-7.6$ MeV. These unobserved levels may significantly enhance the $^{18}$F$+p$ reaction rates, and thus their properties must be determined.

## II. EXPERIMENTAL DETAILS

We have searched for these missing levels in $^{19}$Ne by measuring the $^{1}$H$(^{18}$F$,p)^{18}$F excitation function over the energy range $E_{\mathrm{c.m.}}\simeq0.3-1.3$ MeV. A 24-MeV $^{18}$F beam was used at the ORNL Holifield Radioactive Ion Beam Facility (HRIBF) [13] to bombard a thick 2.8 mg/cm$^2$ polypropylene $CH_2$ target. The $^{18}$F beam was fully stripped to $q=9^+$ in a thin carbon foil before the energy-analyzing magnet of the HRIBF Tandem electrostatic accelerator to remove an unwanted $^{18}$O contamination. Even with use of this unfavorable charge state ($<5\%$ charge state fraction), more than $10^4$ $^{18}$F ion/s were delivered to the target station with 100% purity. The $^{18}$F beam was stopped in the thick target, and scattered protons from the $^{1}$H$(^{18}$F$,p)^{18}$F reaction were detected at $\theta_{lab}=8°-16°$ by a double-sided silicon-strip detector (DSSD). Because the scattered protons lose relatively little energy in the target, measurements of the proton's energy and angle of scatter are sufficient to determine the center-of-mass energy at which the reaction occurred [14,15]. A measurement of the scattered proton energy spectrum at a fixed angle can thus be used to extract the excitation function for the $^{1}$H$(^{18}$F$,p)^{18}$F reaction over a wide range of center-of-mass energies.

Positron decay by the large amount of $^{18}$F implanted in the target material resulted in an intense low-energy background in the DSSD. This background was suppressed by measuring the time difference in a Time-to-Amplitude Converter (TAC) between events in the DSSD and delayed signals from a microchannel plate assembly placed upstream of the target [16]. Scattered protons from the $^{1}$H$(^{18}$F$,p)^{18}$F reaction were cleanly distinguished from decays and other events by plotting the TAC output versus the energy detected in the DSSD (Fig. 1). This low-energy background prevented us from extending the measurement to energies lower than $E_{\mathrm{c.m.}}\simeq0.3$ MeV.

Data were collected in event mode for approximately 62 hours. Events identified as protons were sorted in two-degree angular bins, corrected for energy loss in the target, and are plotted in Fig. 2. The number of counts per channel generally fell with increasing $E_{\mathrm{c.m.}}$, which was simply a manifestation of the Rutherford scattering cross section. There were, however, significant deviations from Rutherford scattering at $E_{\mathrm{c.m.}}=0.665$ MeV and 1.01 MeV where the cross section

 

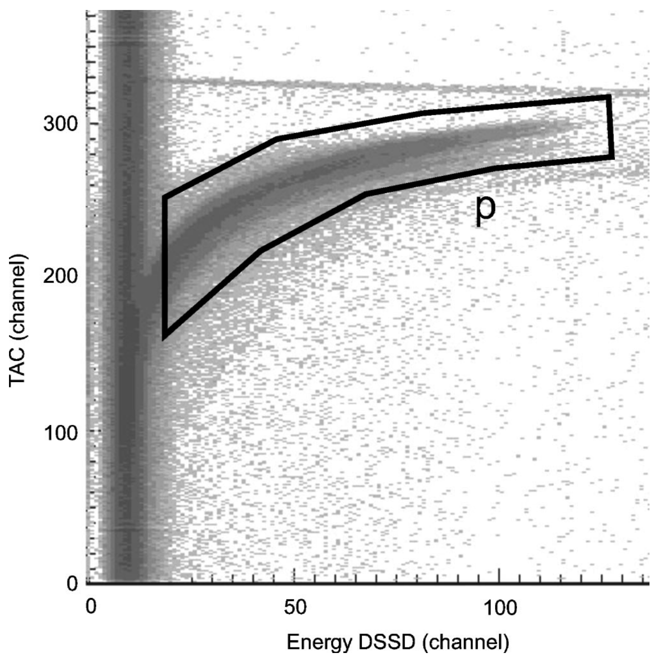


FIG. 1. A TAC was used to measure the time between DSSD events and a delayed microchannel plate signal. This TAC spectrum was plotted against the energy of the detected particle to distinguish protons from other background events.

abruptly rises and falls, respectively. The increase in cross section at $E_{c.m.}=665$ keV arises from the previously observed $J^{\pi}=\frac{3}{2}^{+}$ scattering resonance [9]. Since the properties of this resonance are well known, it provided a convenient internal energy calibration. The sharp fall in cross section

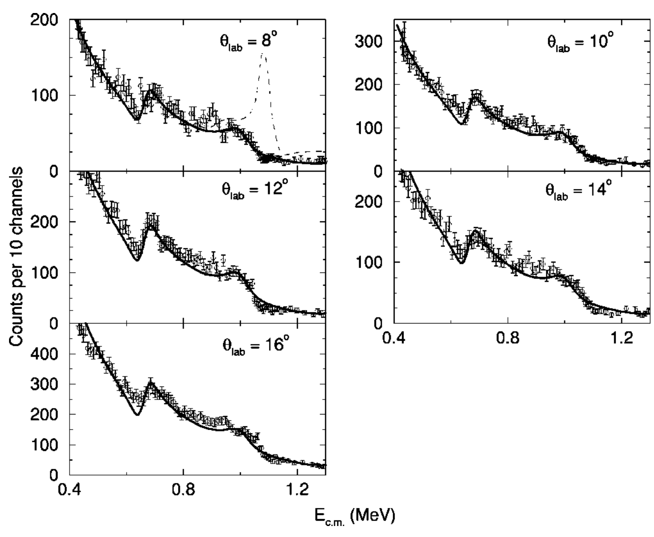


FIG. 2. The proton energy spectra from the $^{1}H(^{18}F,p)^{18}F$ reaction are shown as a function of angle. These data have been corrected for energy loss in the target and internally calibrated by the $E_{c.m.}=665$ keV resonance [9]. The solid line shows the best fit assuming a $\frac{7}{2}^{+}$ resonance at $E_{c.m.}\simeq 1.01$ MeV. The dashed line in the 8° spectrum shows the excitation function expected using the resonance parameters from Ref. [20].

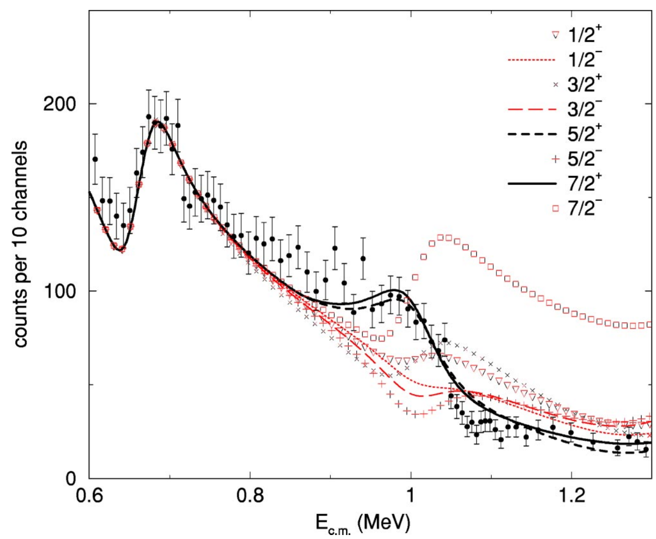


FIG. 3. (Color online) The data from the $^{1}H(^{18}F,p)^{18}F$ reaction measured at $\theta_{lab}=12°$ are shown. The curves show the calculated excitation functions for a variety of spin values for the $E_{c.m.}=1.01$ MeV resonance. Only a $\frac{7}{2}^{+}$ or $\frac{5}{2}^{+}$ assignment is consistent with the data.

near $E_{c.m.}=1.01$ MeV could not be explained using previously-known levels and indicated the presence of a newly-observed $^{19}$Ne resonance.

## III. DATA ANALYSIS

Excitation functions were calculated using the *R*-Matrix code MULTI [17]. A good fit to the data was obtained (see Figs. 2 and 3) using just three resonances: the $J^{\pi}=\frac{3}{2}^{+}$ resonance at $E_{c.m.}=0.665$ MeV, a newly-observed $J^{\pi}=\frac{7}{2}^{+}$ or $\frac{5}{2}^{+}$ resonance near $E_{c.m.}=1.01$ MeV, and a broad *s*-wave resonance higher in energy. The tail of the *s*-wave resonance was needed to reproduce the high-energy ($E_{c.m.}>1.1$ MeV) part of the spectrum, but our fits were relatively insensitive to its properties. A simultaneous fit of the data sets obtained at each angle was performed by varying the properties of the resonance near $E_{c.m.}=1.01$ MeV, and leaving the properties of the known $E_{c.m.}=0.665$ MeV resonance fixed at the values measured in Ref. [9]. For a given set of resonance parameters, the cross section was calculated at each angle using MULTI and then convoluted with the detector resolution. The chi-square was then computed, and the resonance parameters varied until the minimum of the chi-square was found.

The best fit ($\chi^2_{\nu}=1.45$) was obtained for a $J^{\pi}=\frac{7}{2}^{+}$ resonance at $E_{c.m.}=1.009\pm0.014$ MeV ($E_x=7.420\pm0.014$ MeV) with $\Gamma_p=27\pm4$ keV and $\Gamma_{\alpha}=71\pm11$ keV. A fit nearly as good ($\chi^2_{\nu}=1.52$) was obtained for a $J^{\pi}=\frac{5}{2}^{+}$ resonance at the same energy with $\Gamma_p=31\pm4$ keV and $\Gamma_{\alpha}=71\pm11$ keV. As shown in Fig. 3, no other spin and parity assignments were consistent with the data. A $J^{\pi}=\frac{5}{2}^{+}$ assignment, however, appears to be rather unlikely from a comparison with the mirror nucleus, $^{19}$F. The only known candidates (see Fig. 4) for an analog level are the $J^{\pi}=\frac{5}{2}^{+}$ $^{19}$F state at $E_x=7.54$ MeV and the $J^{\pi}=\frac{7}{2}^{+}$ $^{19}$F state at 7.56 MeV [6]. It should be noted that

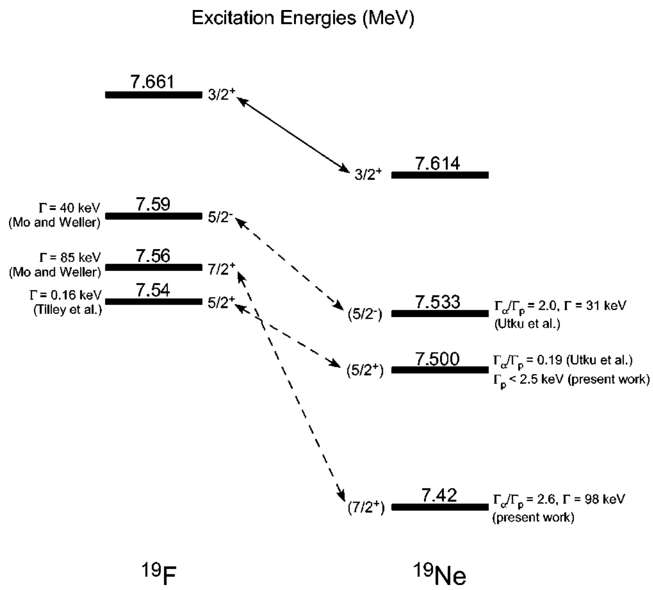


FIG. 4. An updated $^{19}$Ne level scheme is shown along with proposed mirror assignments.

the $^{19}$F state at 7.59 MeV was incorrectly shown in Fig. 6 of Ref. [6] to have $J^\pi = \frac{5}{2}^+$ instead of the measured value of $\frac{5}{2}^-$ [18]. The 7.54 MeV $\frac{5}{2}^+$ $^{19}$F level is narrow ($\Gamma = 0.16$ keV) and is thus not a good candidate for the mirror to our newly-observed level with $\Gamma \simeq 98$ keV. On the other hand, the $\frac{7}{2}^+$ $^{19}$F level is rather broad ($\Gamma = 85$ keV [19]) and has no other obvious analog in $^{19}$Ne. The newly observed $^{19}$Ne level at $E_x = 7.420 \pm 0.014$ MeV is, therefore, most likely the mirror to the $J^\pi = \frac{7}{2}^+$ $^{19}$F level at 7.56 MeV.

In addition to the best fit calculation, we also show in Fig. 2 the calculated excitation function using the $^{19}$Ne resonance parameters from Ref. [20]. That calculation includes contributions from 13 resonances, most of which produce only minor perturbations to the excitation function. The one glaring discrepancy is for the expected contribution from the $\frac{5}{2}^+$ level at $E_{\mathrm{c.m.}} = 1.09$ MeV ($E_x = 7.500$ MeV). This level was observed in Ref. [6] to have $\Gamma_p/\Gamma_\alpha \simeq 5.25$ and a $1\sigma$ upper limit of $\Gamma < 32$ keV. A width of 16 keV was adopted for this level in Ref. [20], but clearly (as seen in Fig. 2) the actual width is much smaller. This is not really surprising considering the width of the proposed analog level is only 0.16 keV [18]. Using the ratio of the proton- to the alpha-partial width measured in Ref. [6], we can set an upper limit on the proton width of $\Gamma_p(7.500 \text{ MeV}) < 2.5$ keV at the 90% confidence level.

Since there are still several ($\lesssim 7$) $^{19}$Ne levels expected in this excitation energy region, we have set upper limits on the proton widths of these missing levels. Resonances of a given spin and parity were added one at a time to the level scheme between $E_{\mathrm{c.m.}} = 0.7$ and 0.9 MeV, and for several alpha widths representative of the known $^{19}$Ne levels ($\Gamma_\alpha = 1-100$ keV), the 90% confidence level upper limits on $\Gamma_p$ were calculated. The results of this procedure are shown in Table I. Within the range $E_{\mathrm{c.m.}} = 0.7-0.9$ MeV, the calculated upper limits were relatively insensitive to the particular energy used in this process. In Table II, we repeat the same procedure at higher energies, $E_{\mathrm{c.m.}} = 1.1-1.3$ MeV. In general the upper limits at these energies are not nearly as stringent because of the reduced statistics. These upper limits are particularly high for low-spin states and states that produce negative deviations from Rutherford scattering (e.g., $J^\pi = \frac{1}{2}^-$ and $\frac{5}{2}^-$).

TABLE I. Upper limits on $\Gamma_p$ are shown for missing levels. Resonances were added at $E_{\mathrm{c.m.}} = 0.7-0.9$ MeV with a variety of alpha widths between 1 and 100 keV. For a given set of trial resonance parameters ($J^\pi, \Gamma_\alpha$), the upper limit on $\Gamma_p$ was computed at the 90% confidence level.

| $J^\pi$ | $\Gamma_\alpha = 1$ keV $\Gamma_p$ (keV) | $\Gamma_\alpha = 10$ keV $\Gamma_p$ (keV) | $\Gamma_\alpha = 100$ keV $\Gamma_p$ (keV) |
|---|---|---|---|
| $\frac{1}{2}^+$ | 2.7 | 1.8 | 1.8 |
| $\frac{1}{2}^-$ | 1.7 | 1.1 | 2.0 |
| $\frac{3}{2}^+$ | 1.4 | 0.7 | 0.5 |
| $\frac{3}{2}^-$ | 0.9 | 0.6 | 1.0 |
| $\frac{5}{2}^+$ | 2.6 | 3.6 | 7.6 |
| $\frac{5}{2}^-$ | 0.6 | 0.4 | 0.8 |
| $\frac{7}{2}^+$ | 1.0 | 0.2 | 0.1 |
| $\frac{7}{2}^-$ | 1.2 | 1.4 | 0.8 |

## IV. ASTROPHYSICAL IMPLICATIONS

The data obtained in this experiment mainly impact our understanding of the high temperature behavior of the $^{18}$F $+p$ reactions, and so the subsequent paragraphs will focus on the rates of these reactions above $T > 1$ GK. The rates of the $^{18}$F$(p,\alpha)^{15}$O and $^{18}$F$(p,\gamma)^{19}$Ne reactions are mostly dominated by the $E_{\mathrm{c.m.}} = 330$ and 665 keV resonances at temperatures below this [8,20,10]. We group together in Table III the properties of known $^{19}$Ne levels above the proton threshold. These values are unchanged from previous papers [8,10,20] except where indicated and described below.

TABLE II. Upper limits on $\Gamma_p$ are shown for missing levels. Resonances were added at $E_{\mathrm{c.m.}} = 1.1-1.3$ MeV with a variety of alpha widths between 1 and 100 keV. For a given set of trial resonance parameters ($J^\pi, \Gamma_\alpha$), the upper limit on $\Gamma_p$ was computed at the 90% confidence level.

| $J^\pi$ | $\Gamma_\alpha = 1$ keV $\Gamma_p$ (keV) | $\Gamma_\alpha = 10$ keV $\Gamma_p$ (keV) | $\Gamma_\alpha = 100$ keV $\Gamma_p$ (keV) |
|---|---|---|---|
| $\frac{1}{2}^+$ | 7.8 | 12.3 | 27.3 |
| $\frac{1}{2}^-$ | 63.8 | 37.2 | 37.1 |
| $\frac{3}{2}^+$ | 4.9 | 11.5 | 27.0 |
| $\frac{3}{2}^-$ | 3.4 | 9.8 | 33.5 |
| $\frac{5}{2}^+$ | 0.6 | 0.8 | 1.5 |
| $\frac{5}{2}^-$ | 1.6 | 3.1 | 15.4 |
| $\frac{7}{2}^+$ | 1.2 | 3.7 | 18.0 |
| $\frac{7}{2}^-$ | 1.0 | 2.6 | 6.9 |

TABLE III. The properties of $^{19}$Ne levels above the proton threshold are tabulated. Much of this information is discussed in previous papers (Refs. [6,8,10,20]) except where indicated. The $\gamma$-widths in brackets were assumed for the purpose of calculating the $^{18}$F$(p,\gamma)^{19}$Ne reaction rate.

| $E_x(^{19}$F) (MeV) | $E_x(^{19}$Ne) (MeV) | $E_{\text{c.m.}}$ (keV) | $J^\pi$ | $\Gamma_\gamma$ (eV) | $\Gamma_p$ (keV) | $\Gamma_\alpha$ (keV) | References |
|---|---|---|---|---|---|---|---|
| 6.497 | 6.419 | 8(6) | $\frac{3}{2}^+$ | 0.85(15) | $4.3(9)\times10^{-37}$ | 0.5(5) | [10,20] |
| 6.429 | 6.437 | 26(9) | $\frac{1}{2}^-$ | [1(1)] | $(2.8^{+5.6}_{-1.9})\times10^{-20}$ | 216(19) | [8,20] |
| 6.528 | 6.449 | 38(7) | $\frac{3}{2}^+$ | 1.2(2) | $6.6(6.6)\times10^{-15}$ | 4.3(3.7) | [10,20] |
| 6.838 | 6.698 | 287(6) | $\frac{5}{2}^+$ | 0.33(6) | $2.5(2.5)\times10^{-5}$ | 1.2(1.0) | [10,20] |
| 6.787 | 6.741 | 330(6) | $\frac{3}{2}^-$ | 5.50(76) | $2.22(69)\times10^{-3}$ | 2.7(2.3) | [8,20] |
| 6.927 | 6.861 | 450(6) | $\frac{7}{2}^-$ | 2.40(35) | $1.6(1.6)\times10^{-5}$ | 3.1(2.7) | [7,20] |
| 7.30 | 7.076 | 664.7(1.6) | $\frac{3}{2}^+$ | [1(1)] | 15.2(1.0) | 23.8(1.2) | [9,10] |
| 7.262 | 7.238 | 827(6) | $\frac{3}{2}^+$ | [1(1)] | 0.35(35) | 6.0(5.2) | This work, [20] |
| 7.364 | 7.253 | 842(10) | $\frac{1}{2}^+$ | [1(1)] | 0.9(9) | 23(20) | This work, [20] |
| 7.560 | 7.420 | 1009(14) | $\frac{7}{2}^+$ | [1(1)] | 27(4) | 71(11) | This work |
| 7.540 | 7.500 | 1089(9) | $\frac{5}{2}^+$ | 5.8(0.9) | 1.25(1.25) | 0.24(24) | This work, [6,20] |
| 7.590 | 7.533 | 1122(11) | $\frac{5}{2}^-$ | [1(1)] | 10(6) | 21(11) | This work, [6,20] |

The $\frac{7}{2}^-$ 450-keV $^{19}$Ne resonance was not listed in Table 1 of Ref. [20] but was included in the reaction rate calculation. Its properties were measured in Ref. [7], but because of its unfavorable spin and parity, it does not contribute significantly to the $^{18}$F$+p$ reaction rates. The proton width of the $\frac{3}{2}^+$ 827-keV resonance was reduced in accordance with the upper limit obtained in this work. The resonance included in Table 1 of Ref. [20] at 915 keV was not considered in this work because of only very weak evidence for its existence [21]. Additionally, there is no evidence for a $^{19}$F level postulated in Ref. [20] to be at $E_x$=7.35 MeV. We, therefore, tentatively link as a mirror pair the $\frac{1}{2}^+$ $^{19}$F level at $E_x$ =7.364 MeV with the $^{19}$Ne level at $E_x$=7.253 MeV. The proton width was then set at a level consistent with the upper limits from this experiment. The properties of the $E_{\text{c.m.}}$ =1009 keV resonance were measured in this work. The proton width of the 1089 keV resonance was set at a level consistent with the upper limit, and then the alpha width scaled by the ratio measured in Ref. [6]. The 1122-keV resonance was tentatively assigned to be the mirror the $\frac{5}{2}^-$ $^{19}$F level at $E_x$=7.590 MeV with properties measured in Ref. [6].

Using the values of resonance parameters in Table III, we have calculated updated $^{18}$F$+p$ reaction rates which are plotted in Fig. 5. The largest contributions to the $^{18}$F$(p,\alpha)^{15}$O rate in the range $T$=1–3 GK come from the 665-keV resonance and the newly-observed 1009-keV resonance. The addition of the 1009-keV resonance increases the $^{18}$F$(p,\alpha)^{15}$O rate by 16%, 63%, and 106% at $T$=1, 2, and 3 GK, respectively. The $^{18}$F$(p,\gamma)^{19}$Ne rate is dominated by the 665-keV resonance below 1.6 GK and the 1089-keV resonance above. The 1009-keV resonance was calculated to increase the rate by ~7% over 1–3 GK. Throughout this temperature range, the $^{18}$F$(p,\alpha)^{15}$O reaction rate is about 3-4 orders of magnitude faster than the $^{18}$F$(p,\gamma)^{19}$Ne rate.

## V. CONCLUSIONS

Knowledge of the $^{19}$Ne level structure is important for calculating the astrophysical rates of the $^{18}$F$(p,\alpha)^{15}$O and $^{18}$F$(p,\gamma)^{19}$Ne reactions. There are approximately eight $^{19}$F levels for which analog $^{19}$Ne levels had not previously been observed but are expected to be in the astrophysically-important excitation energy range, $E_x$=6.4–7.6 MeV. We have searched for these missing levels by measuring the $^{1}$H$(^{18}$F$,p)^{18}$F excitation function from $E_{\text{c.m.}}\simeq$0.3–1.3 MeV. We have identified a new $^{19}$Ne level at $E_x$ =7.420±0.014 MeV. This level has $J^\pi=\frac{7}{2}^+$ or $\frac{5}{2}^+$ with the most likely mirror assignment being that it is the analog to the $\frac{7}{2}^+$ $^{19}$F level at 7.56 MeV. A simultaneous fit to our data

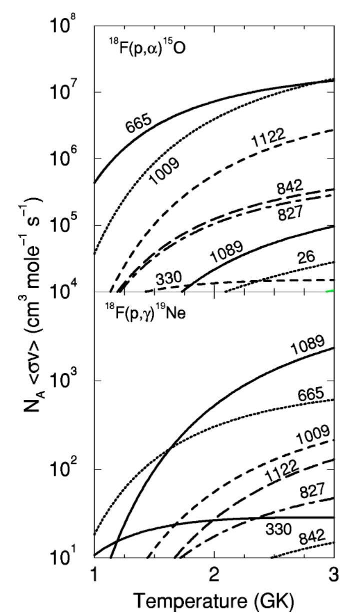


FIG. 5. Updated calculations of the $^{18}$F$(p,\alpha)^{15}$O and $^{18}$F$(p,\gamma)^{19}$Ne reaction rates using resonance parameters from Table III are shown. The high temperature range $T$=1–3 GK is focused on since this range is most relevant for the data taken during this experiment.

resulted in a best fit for $J^{\pi}=\frac{7}{2}^{+}$, $E_x=7.420\pm0.014$ MeV, $\Gamma_p=27\pm4$ keV, and $\Gamma_{\alpha}=71\pm11$ keV.

We can additionally exclude the contribution of an expected $E_x=7.500$ MeV $\frac{5}{2}^{+}$ state at the level calculated in Ref. [20]. We set an upper limit on the proton width of this state at $\Gamma_p<2.5$ keV at the 90% confidence level.

Updated reaction rate calculations demonstrate that the $^{18}$F$(p,\alpha)^{15}$O reaction rate is dominated by contributions from the 665-keV resonance and the newly-observed 1009-keV resonance in the temperature range 1–3 GK. The addition of the 1009-keV resonance increases the $^{18}$F$(p,\alpha)^{15}$O rate by 16%, 63%, and 106% at $T=1$, 2, and 3 GK, respectively. The $^{18}$F$(p,\gamma)^{19}$Ne reaction rate is dominated by contributions from the 665-keV and 1089-keV resonances at $T=1-3$ GK with the 1009-keV resonance increasing the calculated rate by $\sim$7%.

## ACKNOWLEDGMENTS

The authors wish to thank N. Shu for providing useful discussions and the staff of the HRIBF whose hard work made this experiment possible. This research was sponsored by the Laboratory Directed Research and Development Program of Oak Ridge National Laboratory, managed by UT-Battelle, LLC, for the U.S. Department of Energy under Contract No. DE-AC05-00OR22725. This work was also supported in part by the U.S. Department of Energy under Contract No. DE-FG02-96ER40955 with Tennessee Technological University and Contract No. DE-FG02-97ER41041 with the University of North Carolina at Chapel Hill.

[1] M. Hernanz, J. Gómez-Gomar, and J. José, New Astron. Rev. **46**, 559 (2002).
[2] M. J. Harris, J. E. Naya, B. J. Teegarden, T. L. Cline, N. Gehrels, D. M. Palmer, R. Ramaty, and H. Seifer, Astrophys. J. **522**, 424 (1999).
[3] A. Coc, M. Hernanz, J. José, and J.-P. Thibaud, Astron. Astrophys. **357**, 561 (2000).
[4] C. Iliadis, A. Champagne, J. José, S. Starrfield, and P. Tupper, Astrophys. J., Suppl. Ser. **142**, 105 (2002).
[5] A. E. Champagne and M. Wiescher, Annu. Rev. Nucl. Part. Sci. **42**, 39 (1992).
[6] S. Utku *et al.*, Phys. Rev. C **57**, 2731 (1998); **58**, 1354(E) (1998).
[7] D. W. Visser, J. A. Caggiano, R. Lewis, W. B. Handler, A. Parikh, and P. D. Parker, Phys. Rev. C **69**, 048801 (2004).
[8] D. W. Bardayan *et al.*, Phys. Rev. Lett. **89**, 262501 (2002).
[9] D. W. Bardayan *et al.*, Phys. Rev. C **63**, 065802 (2001).
[10] R. L. Kozub *et al.*, Bull. Am. Phys. Soc. **48**, 181 (2003); nucl-ex/0405033.
[11] R. Coszach *et al.*, Phys. Lett. B **353**, 184 (1995).
[12] J.-S. Graulich *et al.*, Phys. Rev. C **63**, 011302(R) (2001).
[13] G. D. Alton and J. R. Beene, J. Phys. G **24**, 1347 (1998).
[14] A. Galindo-Uribarri *et al.*, Nucl. Instrum. Methods Phys. Res. B **172**, 647 (2000).
[15] J. Gómez del Campo *et al.*, Phys. Rev. Lett. **86**, 43 (2001).
[16] D. Shapira, T. A. Lewis, and L. D. Hulett, Nucl. Instrum. Methods Phys. Res. A **454**, 409 (2000).
[17] R. O. Nelson, E. G. Bilpuch, and G. E. Mitchell, Nucl. Instrum. Methods Phys. Res. A **236**, 128 (1985).
[18] D. R. Tilley, H. R. Weller, C. M. Cheves, and R. M. Chasteler, Nucl. Phys. **A595**, 1 (1995).
[19] T. Mo and H. R. Weller, Nucl. Phys. **A198**, 153 (1972).
[20] N.-C. Shu, D. W. Bardayan, J. C. Blackmon, Y.-S. Chen, R. L. Kozub, P. D. Parker, and M. S. Smith, Chin. Phys. Lett. **20**, 1470 (2003), and references therein.
[21] D. S. Haynes, K. W. Kemper, and N. R. Fletcher, Phys. Rev. C **5**, 5 (1972).